Inorg. Chem. **2005**, *44*, 538–545

Diversification of Hydrothermal Reaction Products Induced by Naphthalene Molecules

Eun Young Choi and Young-Uk Kwon*

Department of Chemistry and BK-21 School of Molecular Science, Sungkyunkwan University, Suwon 440-746, Korea

Received July 20, 2004

Hydrothermal reactions in the system of Ni(II), 1,3,5-benzenetricarboxylic acid ($btcH_3$), and 4,4′-bipyridine (bpy) with or without naphthalene produced three new coordination polymers, $[Ni_2(bpy)_3(btcH)_2 \cdot (H_2O)] \cdot (H_2O)$ (**2**), $[Ni_2(bpy)_2(btcH)_2] \cdot (C_{10}H_8)_3$ (**3**), and $Ni(bpy)(btcH_2)_2$ (**4**), in addition to previously reported $[Ni_2(bpy)_2(btcH)_2] \cdot (C_{10}H_8)_{0.75} \cdot H_2O$ (**1**). Polymer **2** is the only product when naphthalene is absent in the reaction, and it is composed of 2D layers of coordination polymers with guest water molecules between them. When naphthalene is added to the system, compounds **1**, **3**, or **4** are formed depending on composition. Compound **3** has a 3D framework structure with naphthalene guests, and **4** has a 1D chainlike structure with no guest. Details of the synthesis condition and crystal structures of each compound are discussed. Crystallographic data: **2**, *C*2/*c*, $a = 22.500(3)$ Å, $b = 20.053(3)$ Å, $c = 19.625(3)$ Å, $\beta = 99.314(3)°$; **3**, $P2_1/c$, $a = 11.248(2)$ Å, $b = 16.801(4)$ Å, $c = 14.945(3)$ Å, $\beta = 103.732(4)°$; **4**, *C*2/*c*, $a = 10.692(2)$ Å, $b = 11.114(3)$ Å, $c = 21.962(5)$ Å, $\beta = 106.268(11)°$

Introduction

Metal-organic framework compounds (MOFs) are a new class of materials that have many potential applications in the areas of catalysis, separation, sorption, sensors, and electronic and magnetic devices.[1−3] They are also very challenging subjects for synthetic chemists because their compositional and structural diversities, which may be tuned by the choice of ligands and metal precursors, lead to the issue of synthesis with a rational design. One of the key elements in the structural design of MOFs is the control of the pores for their shape, size, and symmetry.[4,5]

Among several strategies of the structural design of MOFs in the literature, one stream is incorporating guest molecules within the frameworks, the removal of which often results in porous materials that exhibit interesting behaviors including selective adsorption,[6] structural transformation,[7] and switching of magnetic coupling.[8] Thus far, almost all of the examples of this type of approach have employed low-temperature synthetic routes in nonaqueous solvent systems such as slow diffusion reactions; the guests are polar molecules that are soluble in the solvents. A much larger number of coordination polymers have been synthesized by hydrothermal reactions at high temperatures above 100 °C in water. Although this technique is simpler than the low-temperature routes, most of the compounds show rather

* To whom correspondence should be addressed. E-mail: ywkwon@skku.edu.

(1) (a) Chae, H. K.; Siberio-Pérez, D. Y.; Kim, J.; Go, Y. B.; Eddaoudi, M.; Matzger, A. J.; O'Keeffe, M.; Yaghi, O. M. *Nature* **2004**, *427*, 523. (b) Skoulidas, A. I. *J. Am. Chem. Soc.* **2004**, *126*, 1356. (c) Rosi, N. L.; Eckert, J.; Eddaoudi, M.; Vodak, D. T.; Kim, J.; O'Keeffe, M.; Yaghi, O. M. *Science* **2003**, *300*, 1127.

(2) (a) Tong, M.-L.; Kitagawa, S.; Chang, H.-C.; Ohba, M. *Chem. Commun.* **2004**, 418. (b) Zimmerman, S. C.; Wendland, M. S.; Rakow, N. A.; Zharov, I.; Suslick, K. S. *Nature* **2002**, *418*, 399. (c) Katz, A.; Davis, M. E. *Nature* **2000**, *403*, 286.

(3) (a) Zheng, X.-J.; Li, L.-C.; Gao, S.; Jin, L.-P. *Polyhedron* **2004**, *23*, 1257. (b) Tominaga, M.; Tashiro, S.; Aoyagi, M.; Fujita, M. *Chem. Commun*. **2002**, 2038. (c) Biradha, K.; Fujita, M. *Angew, Chem., Int. Ed*. **2002**, *41* (18), 3392. (d) Evans, O. R.; Lin, W. *Acc. Chem. Res*. **2002**, *35*, 511.

(4) (a) Cui, Y.; Evans, O. R.; Ngo, H. L.; White, P. S.; Lin, W. *Angew. Chem.* **2002**, *114*, 1207. (b) Chand, D. K.; Biradha, K.; Fujita, M.; Sakamoto, S.; Yamaguchi, K. *Chem. Commun*. **2002**, 2486. (c) Pan, L.; Huang, X. Y.; Li, J.; Wu, Y.; Zheng, N. *Angew. Chem., Int. Ed.* **2000**, *39*, 527.

(5) (a) Takamizawa, S.; Nakata, E.-I.; Yokoyama, H.; Mochizuki, K.; Mori, W. *Angew. Chem., Int. Ed*. **2003**, *42*, 4331. (b) Lu, J. Y.; Babb, A. M. *Chem. Commun*. **2002**, 1340.

(6) (a) Dybtsev, D. N.; Chun, H.; Yoon, S. H.; Kim, D.; Kim, K. M. *J. Am. Chem. Soc*. **2004**, *126*, 32. (b) Uemura, K.; Kitagawa, S.; Kondo, M.; Fukui, K.; Kitaura, R.; Chang, H.-C.; Mizutani, T. *Chem. Eur. J*. **2002**, *8*, 3587.

(7) (a) Su, C.-Y.; Goforth, A. M.; Smith, M. D.; Pellechia, P. J.; Zur Loye, H.-C. *J. Am. Chem. Soc.* **2004**, *126*, 3576. (b) Kasai, K.; Aoyagi, M.; Fujita, M. *J. Am. Chem. Soc.* **2000**, *122*, 2140.

(8) (a) Glaser, T. *Angew. Chem., Int. Ed.* **2003**, *42*, 5668. (b) Halder, G. J.; Kepert, C. J.; Moubaraki, B.; Murray, K. S.; Cashion, J. D. *Science* **2002**, *298*, 1762.

10.1021/ic049030j CCC: $30.25
Published on Web 12/31/2004

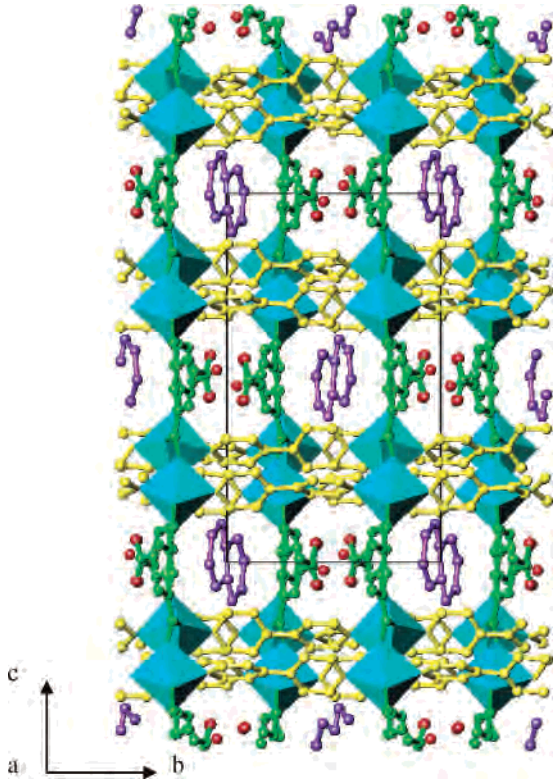

Figure 1. Structure of $[Ni_2(bpy)_2(btcH)_2]\cdot(C_{10}H_8)_{0.75}\cdot(H_2O)$ (**1**) with guest naphthalene (violet) and water molecules (red) viewed along the *a*-axis.

compact structures, often interpenetrated, with no or small void volumes accessible.[9] The contrasting results between the hydrothermal syntheses and the lower temperature ones may be traced to many reasons. An obvious one, we believe, is the large difference between the polarities of water and the organic moieties of the ligands that leads to "phase segregated" states. That is, the organic ligands are in close contact with one another to form densely packed structures.

In an effort to create pores in MOFs, we have considered adding hydrophobic molecules into the hydrothermal systems so that the phase segregation may drive the hydrophobic molecules into the spaces between the ligands and widen up the pores. By this method, we have previously synthesized a MOF with benzene guest molecules. This MOF exhibited size and shape selective sorption properties for benzene and cyclohexene against other ring compounds.[10] Recently, we have communicated on a new MOF with naphthalene and water guests, $Ni_2(bpy)_2(btcH)_2\cdot C_{10}H_8\cdot H_2O$ (**1**, bpy = 4,4′-bipyridine, btc = 1,3,5-benzenetricarboxylic acid) (see Figure 1).[11] In the present study, we have undertaken an extensive study on this Ni^{2+}−bpy−btc−naphthalene system, and obtained three new compounds depending on the reaction composition. Each one of these compounds has a unique feature and different implication on the role of the added naphthalene.

(9) (a) Thirumurugan, A.; Natarajan, S. *Solid State Sci.* **2004**, *6*, 599. (b) Tong, M.-L.; Chen, X.-M.; Batten, S. R. *J. Am. Chem. Soc.* **2003**, *125*, 16170. (c) Wu, C.-D.; Lu, C.-Z.; Lu, S.-F.; Zhuang, H.-H.; Huang, J.-S. *Inorg. Chem. Commun.* **2002**, *5*, 171.

(10) Choi, E. Y.; Park, K. S.; Yang, C. M.; Kim, H. J.; Son, J. H.; Lee, S. W.; Lee, Y. H.; Min, D. W.; Kwon, Y.-U. *Chem. Eur. J.* **2004**, *10*, 5535.

(11) Choi, E. Y.; Kwon, Y.-U. *Inorg. Chem. Commun.* **2004**, *7*, 942.

Experimental Section

General Methods. All chemicals purchased were of reagent grade and used without further purification. Elemental analyses (C, H, and N) were performed on an EA1110 elemental analyzer. Fourier transform infrared spectra were obtained with a Nicolet 1700 FT-IR spectrometer using KBr disks dispersed with sample powders in the 4000−400 cm^{-1} range. Thermal gravimetric TG analyses were conducted on a TA4000/SDT 2960 instrument in flowing N_2 with a heating rate of 10 °C min^{-1}.

Hydrothermal Syntheses. $[Ni_2(bpy)_3(btcH)_2(H_2O)]\cdot H_2O$ (2). Compound **2** was synthesized from the reaction mixture of $NiSO_4\cdot 6H_2O$ (1 mmol), 4,4′-bipyridine (1 mmol), 1,3,5-benzenetricarboxylate (0.5 mmol), and H_2O (6 mL) in a 50 mL Teflon-lined autoclave under an autogenous pressure at 180 °C for 4 days, followed by quenching in cold water to room temperature. The product was filtered, washed with distilled water and ethanol, and air-dried at room temperature. The product is blue plate crystals and is insoluble in water and common organic solvents. Anal. Found: C, 55.8%; H, 3.5%; N, 8.1%. Calcd for $C_{48}H_{30}N_6O_{14}Ni_2$: C, 55.6%; H, 3.3%; N, 8.1%. Selected FT-IR data (cm^{-1}): 3440-(m), 1724(s), 1612(s), 1543(m), 1372(s), 1228(w), 1155(m), 1077(w), 810(m), 720(m), 637(m), 452(m), 417(w). TG data show a weight loss of 3% (calcd 2%) at 60−214 °C corresponding to the loss of guest water and coordinated water molecules, followed by a weight loss at 320−500 °C for the decomposition of the organic parts.

$[Ni_2(bpy)_2(btcH)_2]\cdot(C_{10}H_8)_3$ (3). Compound **3** was synthesized from the reaction mixture of $NiSO_4\cdot 6H_2O$ (0.5 mmol), 4,4′-bipyridine (0.5 mmol), 1,3,5-benzenetricarboxylate (1 mmol), naphthalene (1 mmol), and H_2O (6 mL) in a 50 mL Teflon-lined autoclave under autogenous pressure at 180 °C for 4 days, followed by quenching to room temperature. The product was filtered, washed with distilled water, ethanol, and acetone and air-dried at room temperature. The product is pale green needle crystals and is insoluble in water and common organic solvents. Anal. Found: C, 66.1%; H, 3.9%; N, 4.6%. Calcd for $C_{68}H_{46}N_4O_{12}Ni_2$: C, 66.5%; H, 3.8%; N, 4.6%. Selected FT-IR data (cm^{-1}): 3441(s), 1724(m), 1625(s), 1559(m), 1380(s), 1242(w), 1176(m), 1094(m), 789(m), 675(m), 469(m), 413(m). TG data show a weight loss of 9.7% (calcd 10.4%) at 132−215 °C corresponding to the release of naphthalene guest molecule, followed by the decomposition of the organic part up to 531 °C.

$Ni(bpy)(btcH_2)_2$ (4). Compound **4** was synthesized from the reaction mixture of $NiSO_4\cdot 6H_2O$ (1 mmol), 4,4′-bipyridine (1 mmol), 1,3,5-benzenetricarboxylate (1 mmol), naphthalene (1 mmol), and H_2O (6 mL) in a 50 mL Teflon-lined autoclave under autogenous pressure at 180 °C for 4 days, followed by quenching to room temperature. The resultant pale green block crystals were hand-picked, washed with distilled water, ethanol, and acetone and air-dried at room temperature. Anal. Found: C, 53.0%; H, 2.9%; N, 4.3%. Calcd for $C_{28}H_{18}N_2O_{12}Ni_2$: C, 53.1%; H, 2.9%; N, 4.4%. Selected FT-IR data (cm^{-1}): 3443(m), 1734(s), 1700(s), 1610(s), 1545(m), 1422(s), 1273(m), 1207(s), 1161(s), 1112(s), 821(w), 741(w), 663(m), 491(w), 456(w), 413(w). TG data show that the weight loss due to the decomposition of the organic ligands starts from 370.1 to 616 °C by 88%.

X-ray Crystallography. Single crystals of **2** and **3** of dimensions 0.4 × 0.2 × 0.05 mm^3 and 0.6 × 0.30 × 0.25 mm^3, respectively, were glued on fibers. Crystal and intensity data were collected at 293(2) K (173(2) K for **3**) using a Siemens 1K CCD diffractometer with graphite-monochromated Mo Kα radiation (0.71073 Å). A hemisphere of reflection data was collected as ω-scan frames with

Table 1. Crystallographic Data and Structure Refinements of **2**, **3**, and **4**

	2	**3**	**4**
empirical formula	$C_{96}H_{64}N_{12}Ni_4O_{28}$	$C_{68}H_{48}N_4Ni_2O_{12}$	$C_{28}H_{18}N_2NiO_{12}$
fw	2068.43	1230.52	633.15
space group	*C*2/*c*	$P2_1/c$	*C*2/*c*
a (Å)	22.500(3)	11.248(2)	10.692(2)
b (Å)	20.053(3)	16.801(4)	11.114(3)
c (Å)	19.625(3)	14.945(4)	21.962(5)
α (deg)	90	90	90
β (deg)	99.314(3)	103.732(4)	101.699(17)
γ (deg)	90	90	90
V (Å^3)	8738(2)	2743(10)	2555.4(10)
Z	4	2	4
T (K)	293(2)	173(2)	296(2)
ρ_{calc} (g cm^{-3})	1.572	1.487	1.646
μ (mm^{-1})	0.942	0.760	0.835
F(000)	4240	1268	1296
reflns collected/ indep reflns	25556/10262	16229/6518	2376/2247
R1 ($I > 2\sigma(I)$)[a]/ wR2[b]	0.0610/0.1583	0.1030/0.2684	0.0325/0.0896

[a] $R1 = \sum||F_o| - |F_c||/\sum F_o$. [b] $wR2 = \{\sum[w(F_o^2 - F_c^2)^2]/\sum[w(F_o^2)^2]\}^{1/2}$.

a width of 0.3°/frame and exposure time of 20 s/frame. Cell parameters were determined and refined by the SMART program.[12] Data reduction was performed using SAINT software, which corrects for Lorentz and polarization effects.[13] Empirical absorption correction was applied with the SADABS program.[14] A block shaped crystal of **4** of approximate dimension 0.79 × 0.71 × 0.22 mm^3 was glued on a glass fiber. X-ray data were collected on a Siemens P4 diffractometer equipped with a Mo X-ray tube and a graphite-monochromator. Intensity data were empirically corrected for absorption with $\psi-$scan data. All calculations were carried out with the use of SHELXTL programs. The positional parameters of the metal atoms and most oxygen atoms were determined by the direct methods or Patterson method (SHELXS-97).[15] Several cycles of refinement and difference Fourier syntheses (SHELXL-97) revealed the other atoms including those of the lattice water and naphthalene molecules.[16] All non-hydrogen atoms were refined anisotropically. All hydrogen positions were program-generated and refined with the riding model. The crystal data and structure refinement results of compounds **2**, **3**, and **4** are summarized in Table 1. Selected bond lengths and angles of compounds **2**, **3**, and **4** are listed in Tables 2, 3, and 4, respectively. The crystal structures of **2** and **3** turn out to have guest molecules entrapped within pores. The pore volumes of the frameworks were calculated by using the program *PLATON*; the guest molecules were omitted in these calculations.

Results and Discussion

Crystal Structures. The crystal structures show that all three compounds **2**−**4** are coordination polymers of Ni^{2+} interconnected by bpy and btc ligands: **2** is a 2D MOF with entrapped guest water molecules, **3** is a 3D MOF with entrapped naphthalene molecules, and **4** has a 1D chainlike structure with no guests. While the bpy ligand functions as a bidentate linker between two Ni^{2+} in all cases, the btc species are bidentate $[btcH]^{2-}$ (in **2**), tridentate $[btcH]^{2-}$ (in **1** and **3**), and monodentate $[btcH_2]^-$ to metals (in **4**) as shown in Chart 1.

$[Ni_2(bpy)_3(btcH)_2(H_2O)]\cdot(H_2O)$ (2). The structure of **2** can be described as a framework that consists of two types of Ni centers (Figure 2a,b). One type of Ni^{2+} ions (Ni(1)) is coordinated by three oxygen atoms from two $btcH^{2-}$ (one bidentate and the other monodentate) ligands and one oxygen atom from a water molecule and two nitrogen atoms from bpy to complete a distorted octahedral coordination environment. The coordination environment of the second type of Ni^{2+} ion (Ni(2)) is similar to that of Ni(1) except that they are bonded to one nitrogen atom from a bpy instead of one oxygen atom from an aqua ligand. This bpy acts as a bridge between the two Ni centers (Ni(1) and Ni(2)) along the *a*-axis, and btc also acts as a bridge between Ni(1) and Ni(2) along the *b*-axis as shown Figure 2a. Only three out of six carboxylate oxygens in the 1,3,5-$btcH^{2-}$ are coordinated to the nickel atom; two oxygens (O1 and O2; O4 and O5) of those three oxygens are coordinated to the nickel metal in a bidentate mode, and one oxygen (O3 and O6) is coordinated to nickel metal in a monodentate mode (Chart 1a). The noncoordinating three oxygen atoms are engaged in hydrogen bonds with guest water molecules.

The two types of nickel ions are interconnected by bpy and btc ligands to form a 2D square grid layer parallel to the *ab*-plane of the monoclinic unit cell (Figure 3a). Rotation of a layer (green in Figure 3) around a 2-fold rotation axis at (0, *y*, $^1/_4$) generates the next (yellow) layer. Inversion of these two layers around an inversion center at (0.5, 0.5, 0.5) generates the other two (purple and blue) layers (Figure 3b). These layers are held by hydrogen bonds between the oxygen atoms of the $btcH^{2-}$ ligands and the guest water molecules in the pores. This pore has a dimension 7.0 × 4.4 Å^2 and has two water molecules (see Table 2and Figure 3a). Omitting these water molecules, the pore volume of **2** is calculated to be 1.4% of the total volume.

$[Ni_2(bpy)_2(btcH)_2]\cdot(C_{10}H_8)_3$ (3). The fundamental building unit of the crystal structure is shown in Figure 4. It is composed of two symmetry-related Ni^{2+} centers that are bridged by two carboxylate groups (O3, O4) of two symmetry-related $btcH^{2-}$ ligands. In addition, each nickel atom is coordinated by two oxygen atoms (O1, O2) from another $btcH^{2-}$ ligand in a bidentate fashion at the equatorial position and two nitrogen atoms (N1, N2) from 4,4′-bpy ligands at the axial positions to complete a slightly distorted octahedral coordination environment. The Ni···Ni distance is 4.35 Å, similar to other dinuclear compounds reported.[17]

The framework can be described as layers, parallel to the *ac*-plane of the monoclinic unit cell, of the dinickel cores

(12) *SMART*, version 5.0, data collection software; Bruker AXS, Inc.; Madison, WI, 1998.
(13) *SAINT*, version 5.0, data intergration software; Bruker AXS, Inc.: Madison, WI, 1998.
(14) Sheldrick, G. M. *SADABS, A program for absorption correction with the Bruker SMART system*; Universitat Göttingen: Göttingen, Germany, 1996.
(15) Sheldrick, G. M. *SHELXS-97*; University of Göttingen: Göttingen, Germany, 1997.
(16) Sheldrick, G. M. *SHELXL-97*; University of Göttingen: Göttingen, Germany, 1997.
(17) (a) Shi, Q.; Cao, R.; Sun, D.-F.; Hong, M.-C.; Liang, Y.-C. *Polyhedron* **2001**, *20*, 3287. (b) Li, Y. G.; Zhang, H.; Wang, E.; Hao, N.; Hu, C.; Yu, Y.; Hall, D. *New. J. Chem.* **2002**, *26*, 1619.

Table 2. Selected Bond Lengths [Å] and Angles [deg] for **2**

Ni(1)−O(1)	2.115(3)	Ni(2)−O(4)	2.184(3)
Ni(1)−O(2)	2.119(3)	Ni(2)−O(5)	2.084(3)
Ni(1)−O(3)	2.022(3)	Ni(2)−O(6)	2.013(3)
Ni(1)−N(1)	2.085(4)	Ni(2)−N(2)	2.096(4)
Ni(1)−N(3)	2.091(4)	Ni(2)−N(4)	2.098(3)
Ni(1)−OW1	2.067(3)	Ni(2)−N(9)	2.100(4)
O(3)−Ni(1)−N(1)/OW1	89.52(14)/95.98(13)	O(4)−Ni(2)−N(4)/N(9)	85.12(12)/156.50(14)
N(1)−Ni(1)−O(1)/OW1	86.82(14)/87.73(14)	O(4)−Ni(2)−N(2)/O(5)	88.90(12)/61.58(11)
O(1)−Ni(1)−O(3)/OW1	159.12(12)/104.40(13)	O(5)−Ni(2)−N(2)/O(6)	89.15(14)/159.11(12)
O(2)−Ni(1)−O(3)/N(1)	97.35(12)/86.88(13)	O(6)−Ni(2)−N(2)/ N(4)	90.06(14)/90.45(14)
O(2)−Ni(1)−O(1)/OW1	61.95(11)/165.57(13)	O(6)−Ni(2)−N(9)	105.52(15)
N(3)−Ni(1)−O(3)/N(1)	91.55(14)/178.83(16)	N(2)−Ni(2)−N(4)/N(9)	174.02(13)/86.61(14)
N(3)−Ni(1)−O(1)/O(2)	92.01(14)/92.51(13)	N(4)−Ni(2)−N(9)	98.99(14)
OW1−Ni(1)−N(3)	92.63(14)	O(5)−Ni(2)−N(9)	95.27(13)
OW1···O(7)	2.54	OW2···O(10)	2.73
OW2···O(8)	2.76	OW2···O(12)	2.67

Table 3. Selected Bond Lengths [Å] and Angles [deg] for **3**[a]

Ni(1)−O(1)	2.190(5)	Ni(1)−O(4)	2.024(5)
Ni(1)−O(2)	2.113(5)	Ni(1)−N(1)	2.077(5)
Ni(1)−O(3)	2.018(4)	Ni(1)−N(2)	2.077(6)
O(1)−Ni(1)−O(2)/O(3)	60.84(16)/157.93(18)	O(4)−Ni(1)−O(1)/O(3)	93.80(17)/107.96(19)
O(1)−Ni(1)−N(1)/N(2)	91.11(19)/88.8(2)	N(1)−Ni(1)−O(3)/O(4)	91.2(2)/93.4(2)
O(2)−Ni(1)−O(3)/O(4)	97.15(18)/154.27(17)	N(2)−Ni(1)−O(3)/O(4)	88.6(2)/87.2(2)
O(2)−Ni(1)−N(1)/N(2)	91.6(2)/87.9(2)	N(1)−Ni(1)−N(2)	179.4(2)
CN1−CN2/CN3	1.413(12)/1.359(12)	CN5−CN4/CN9	1.345(14)/1.395(16)
CN2−CN4/CN6	1.414(12)/1.430(12)	CN6−CN8	1.413(13)
CN10−CN3/CN8	1.391(13)/1.377(14)	CN7−CN6/CN9	1.426(13)/1.354(15)
CN11− CN12/ CN13	1.410(15)/1.416(15)	CN13− CN14	1.33(2)
CN11− CN11#6	1.426(19)	CN14− CN15#6	1.38(2)
CN12− CN15	1.357(19)	CN15− CN14#6	1.38(2)
CN2− CN1− CN3/CN8	120.5(9)/118.7(8)	CN5− CN4−CN2	121.1(9)
CN1− CN2− CN4/CN6	122.5(9)/118.8(8)	CN7−CN6−CN2/CN8	117.6(8)/123.7(9)
CN4− CN 2- CN6	118.7(8)	CN10− CN8− CN6	120.4(10)
CN1− CN3− CN10	121.2(9)	CN8− CN10− CN3	120.2(9)
CN4− CN 5- CN9	121.1(9)	CN9− CN7− CN6	121.4(10)
CN7− CN9− CN5	120.1(10)	CN12−CN11−CN11#6	119.5(12)
CN12− CN11− CN13	122.9(11)	CN15− CN12− CN11	119.2(12)
CN13− CN11−CN 11#6	117.5(13)	CN14− CN13− CN 11	121.0(12)
CN13− CN14−CN 15#6	121.1(12)	CN12−CN15−CN14#6	121.5(13)

[a] Symmetry transformations used to generate equivalent atoms: #1 $-x+2, -y+2, -z$ and #6 $-x+1, -y, -z+1$.

Table 4. Selected Bond Lengths [Å] and Angles [deg] for **4**[a]

Ni(1)−O(1)/O(1)#1	2.1523(15)	Ni(1)−N(1)	2.042(2)
Ni(1)−O(2)/O(2)#1	2.0743(15)	Ni(1)−N(2)	2.021(2)
O(1)−Ni(1)−N(1)/N(2)	90.05(4)/89.95(4)	O(2)#1−Ni(1)−O(1)/O(2)	62.06(6)/177.98(7)
O(1)−Ni(1)−O(1)#1/O(2)	179.89(7)/117.94(6)	N(2)−Ni(1)−O(1)#1	89.95(4)
O(2)−Ni(1)−N(1)/N(2)	88.99(4)/91.01(4)	N(1)−Ni(1)−O(1)#1	90.05(4)
N(1)−Ni(1)−N(2)	180	O(2)#1−Ni(1)−O(1)#1	117.94(6)
		O(2)−Ni(1)−O(1)#1	62.06(6)
O(5)···O(6)#5	2.69	O(5)#5···O(6)	2.69
O(3)···O(5)	2.69	O(2)···O(6)	2.68

[a] Symmetry transformations used to generate equivalent atoms: #1 $-x+1, y, -z+{}^{3}/_{2}$ and #5 $-x, -y, -z$.

that are interconnected by $btcH^{2-}$ ligands. Each $btcH^{2-}$ ligand here connects three nickel atoms, two from a dinickel core (as a μ_2-bridge) and the third from an adjacent dinickel core (as a bidentate chelate) (Chart 1a). These layers are stacked along the *a* direction, and the layers are linked by the bpy ligands. Between the layers and the bpy linkers are two types of pores with dimensions 8.24×6.11 Å^2 and 9.00×9.06 Å^2, each occupied by a naphthalene molecule as shown Figure 5a. These naphthalene molecules show $\pi-\pi$ interaction with bpy ligands of the framework, with the C−C separation between them in the range 3.8−4.0 Å.[18] Omitting the naphthalene molecules, the pore volume of the framework is calculated to be 49.0% of the total volume.

Previously, we reported a similar MOF, **1**. This compound has a similar composition as **3** and has the same dinickel core basic building unit as **3**. Furthermore, both compounds have naphthalene guests. However, they also show some distinct features: (1) Compound **3** has a 3-D framework while **1** has a 2-D framework. (2) Compound **3** has only hydrophobic pores for naphthalene molecules, but **1** has both

(18) Evans, R. C. *An Introduction to Crystal Chemistry*, 2nd ed.; Cambridge University Press: New York, 1966; p 386.

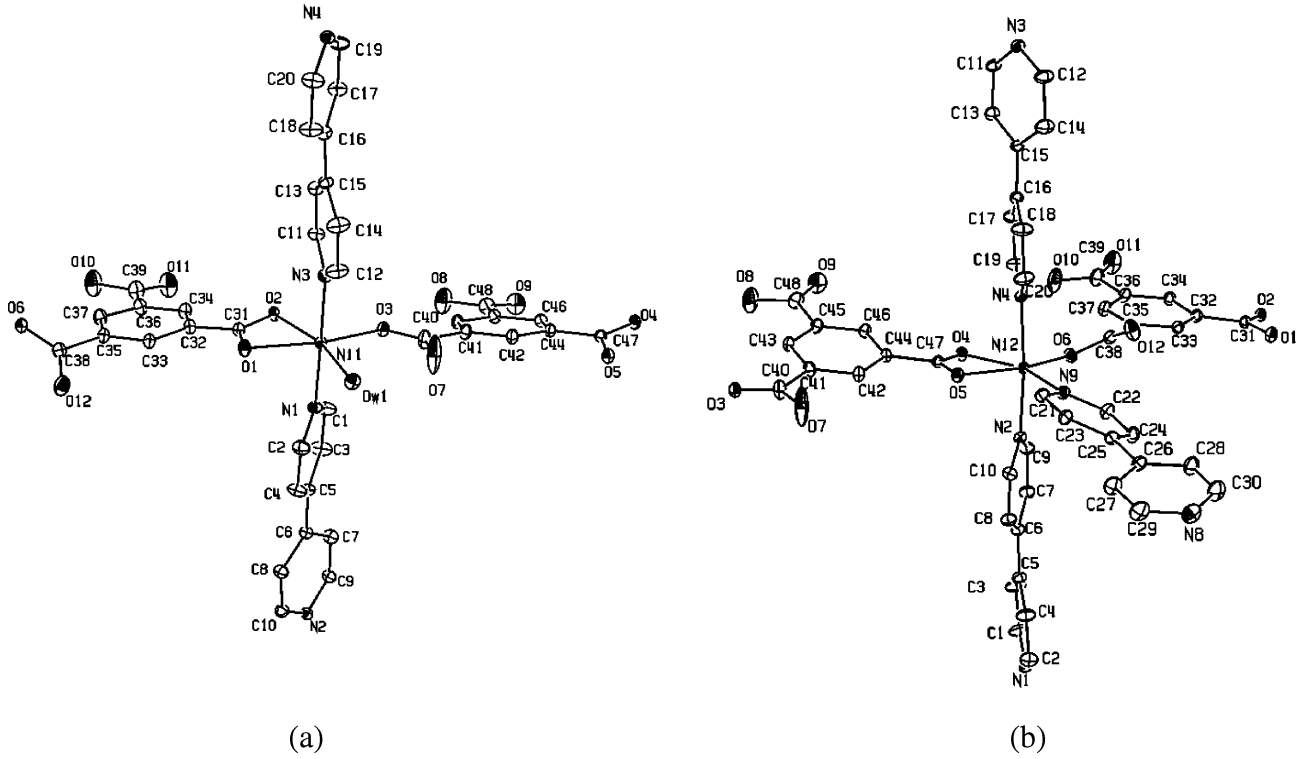

Figure 2. ORTEP drawings of the local coordination environments of nickel centers in $[Ni_2(bpy)_3(btcH)_2(H_2O)]\cdot(H_2O)$ (**2**) around Ni1 (a) and Ni2 (b) with atoms represented by 20% thermal ellipsoids. Hydrogen atoms are omitted for clarity.

Chart 1. Coordination Mode of 1,3,5-btc Ligand in Complexes (a) **2**, (b) **1** and **3**, (c) **4**

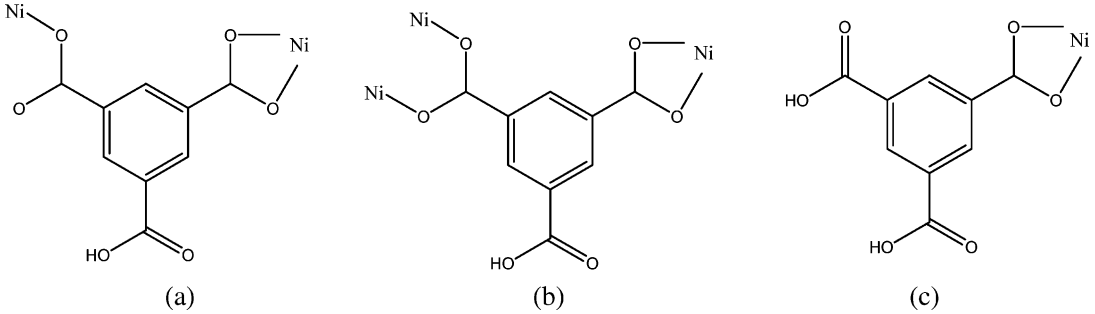

hydrophilic and hydrophobic pores that are filled by water and naphthalene, respectively. (3) Although the guest naphthalene molecules are stabilized by $\pi-\pi$ interaction with the aromatic rings in both compounds, the interacting ligand and modes in **1** and **3** are different. In **1**, the ring planes of naphthalene and the two btc species above and below are parallel to one another as in most of the reported MOFs with aromatic guests.[19] On the other hand, in **3**, there are two types of naphthalene guests, and their planes are tilted from those of interacting bpy rings.

$[Ni(bpy)(btcH_2)_2]$ (4). The coordination environment around Ni^{2+} in **4** is shown in Figure 6a. The Ni^{2+} atom is coordinated by four oxygen atoms from two $btcH_2^-$ ligands in a bidentate mode in the equatorial positions and two nitrogen atoms from two bpys in the axial positions to complete an octahedron. The nickel centers are connected to the next ones through the bpy ligands to form a 1D chain along the *b*-direction of the monoclinic unit cell. Interestingly, the $btcH_2^-$ ligands do not function as a linker between nickel atoms. Rather, they form hydrogen bonds to other $btcH_2^-$ ligands of neighboring chains with relatively short O···O distances of 2.68 Å on average.

Effect of Naphthalene on the Synthesis. The present hydrothermal system of Ni^{2+}, btc, bpy, and naphthalene produced a total of four different coordination polymer compounds whose frameworks are all composed of Ni^{2+}- and btc and bpy ligands. While varying the composition of the reaction mixture in pure water produced **2** as the exclusive product with varied yields, the addition of naphthalene in this system induced a remarkable variety by producing novel compounds **1** and **3** with naphthalene guest molecules and a new compound **4**, depending on the reagent composition.

In general, the MOF compounds from hydrothermal conditions tend to have small pores unless specially designed secondary building units are used.[20] This is a sharp contrast to the many examples of MOF compounds with large pores

(19) Luo, J.; Hong, M.; Wang, R.; Cao, R.; Han, L.; Yuan, D.; Lin, Z.; Zhou, Y. *Inorg. Chem.* **2003**, *42* (15), 4486.

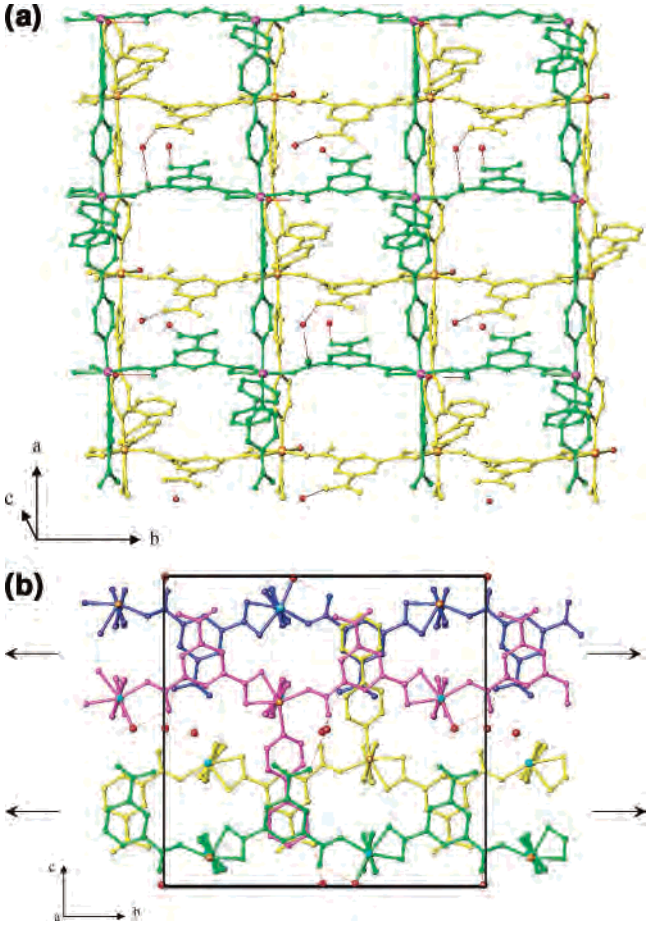

Figure 3. Framework structure of $[Ni_2(bpy)_3(btcH)_2(H_2O)]\cdot(H_2O)$ (**2**) viewed along the *c*-axis (a) and *a*-axis (b). The framework is composed of nickel (pink and orange), bpy, and btc ligands. Red spheres are oxygen atoms of guest water, and red dashed lines are their hydrogen bonds. The arrows in part b are symmetry elements.

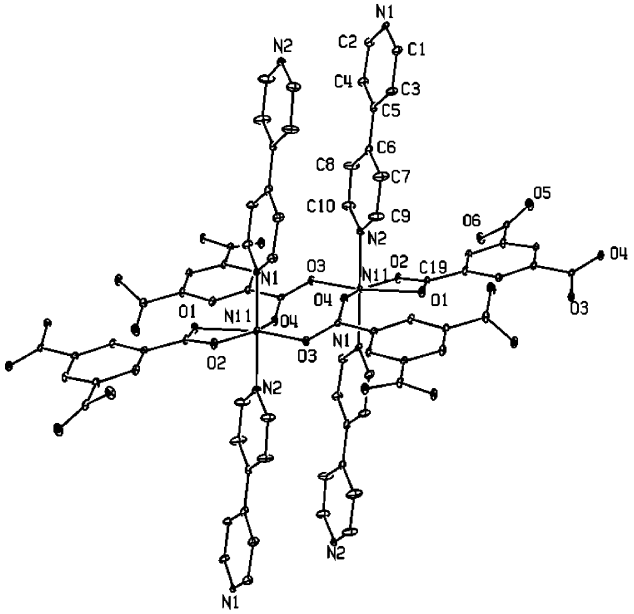

Figure 4. ORTEP drawing of the building block unit of $[Ni_2(bpy)_2(btcH)_2]\cdot(C_{10}H_8)_3$ (**3**) with atoms represented by 20% thermal ellipsoids. Hydrogen atoms are omitted for clarity.

or entrapped guest molecules from lower temperature syntheses that usually employ nonaqueous solvents.[21] There

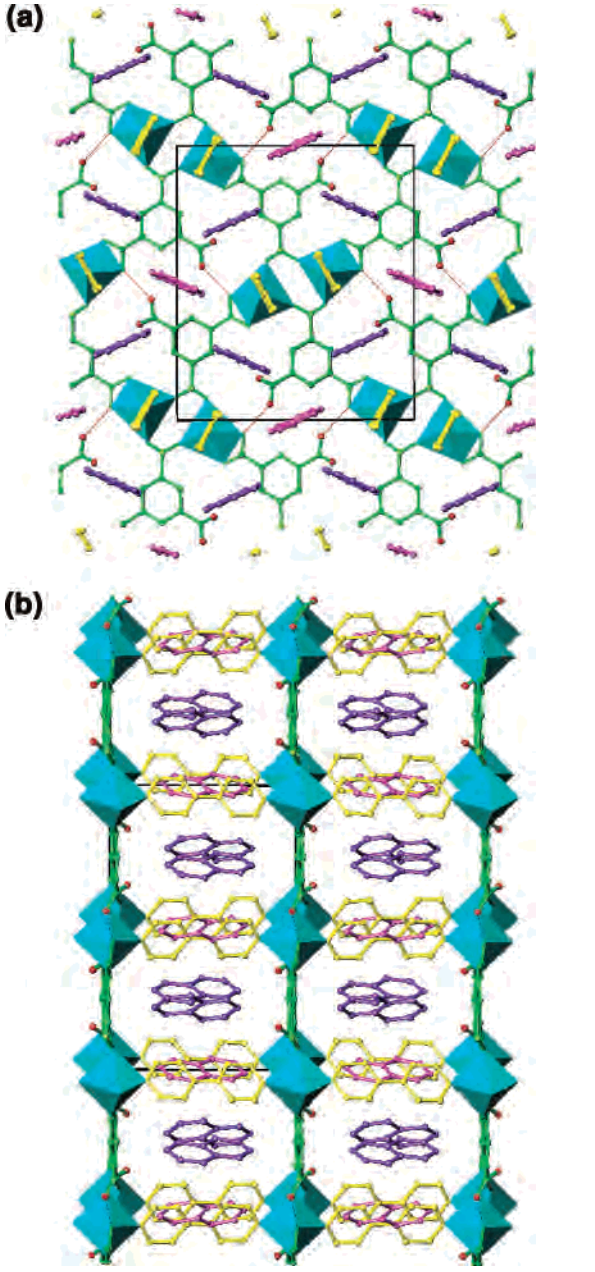

Figure 5. Structure of $[Ni_2(bpy)_2(btcH)_2]\cdot(C_{10}H_8)_3$(**3**) viewed along *a*-axis (a) and *c*-axis (b). Two types of naphthalene molecules are shown in purple and violet. The hydrogen bonds around guest water molecules are represented by dashed lines.

may be several reasons for this contrast, and we believe that the nature of solvent and the pressure are the key factors. The pore walls of most MOFs are composed of the hydrophobic organic parts of the ligands. In the hydrothermal conditions, these (potential) pores tend to be small to minimize the unfavorable contacts between water and the organic ligands. The high pressure condition of hydrothermal reactions also facilitates this "phase segregation" because of the positive partial molar volume of mixing of a hydrophobic molecule with water. In the lower temperature syntheses, these effects are significantly reduced enabling MOFs with large pores.[22] These reasonings can explain why the addition of naphthalene in the reaction results in MOFs **1** and **3** with entrapped naphthalene molecules.

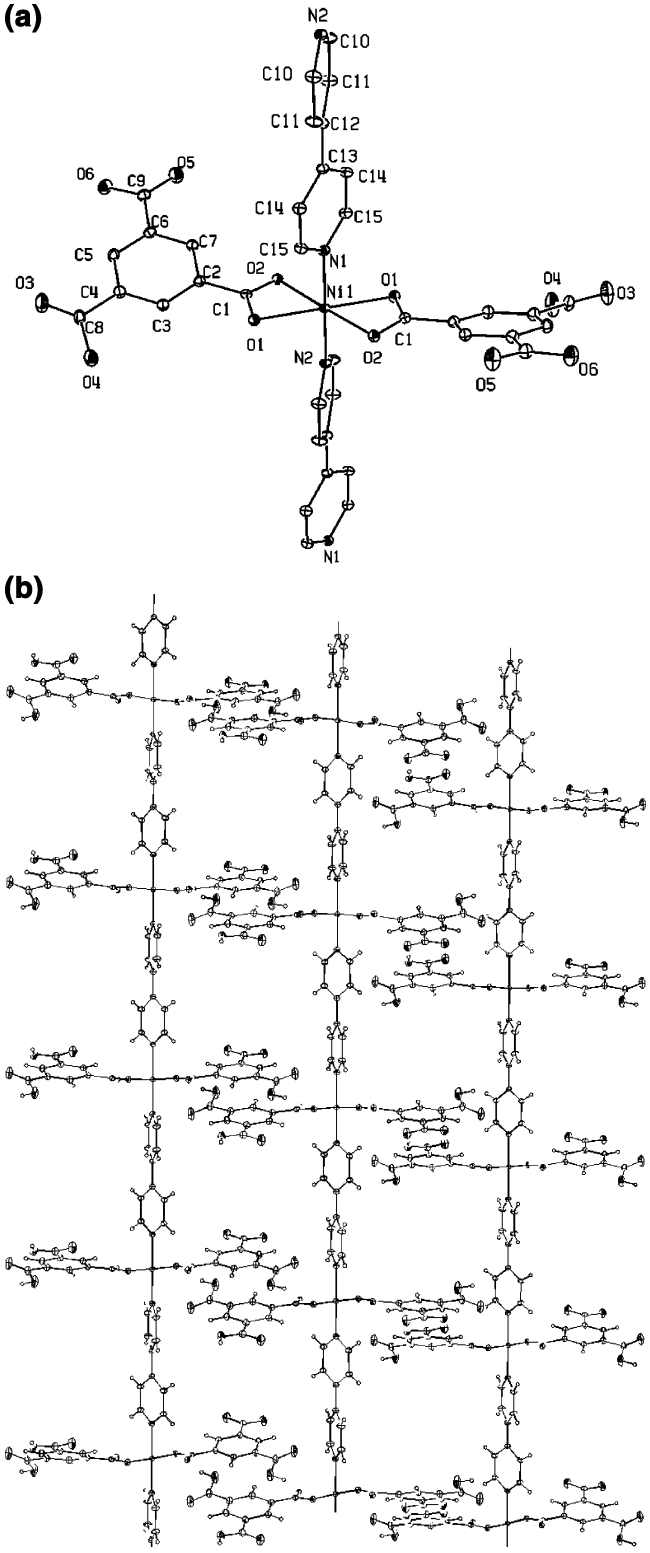

Figure 6. (a) ORTEP drawings of the local coordination environment of a nickel center (a) and of the extended network of [Ni(bpy) ($btcH_2$)$_2$] (**4**) (b) with atoms represented by 20% thermal ellipsoids. Hydrogen atoms are omitted for clarity.

The formation of compound **4** with no naphthalene from a naphthalene-containing reaction suggests that naphthalene molecules have another role during the compound formation. Our experience tells us that the presence of naphthalene is a prerequisite for this compound to form; reactions under similar conditions but without naphthalene all produced compound **2**. The changes of the physical properties, such as dielectric constant or hydrophobicity of the solvent by the dissolution of naphthalene, may be responsible for these observations. However, considering the very low solubility of naphthalene in water of 3.44×10^1 mg/L,[23] such explanation does not seem to be sufficient. The starting mixtures of $NiSO_4 \cdot 6H_2O$, bpy, and btc in water appeared like thick emulsions, which implied the formation of micelles or forms. According to the literature,[24] micelles increase the apparent solubility of nonionic organic compounds (i.e., naphthalene, phenanthrene, etc.). Therefore, naphthalene molecules may be soluble beyond the reported value and influence the phase to be formed by interacting with the reagent molecules during the bond breaking and forming processes.

With the idea of creating pores by hydrophobic interactions between guest molecules and the ligands, we have undertaken many exploratory syntheses with other hydrophobic molecules in the place of naphthalene in the present system. However, the reactions, with benzene, toluene, cyclohexane, pyrene, or anthracene, all produced guest-free **2** or **4** as the only crystalline product. The formation of **4** from these reactions indicates that these molecules also influence the physical properties of water to some extent. In our previous paper on a benzene-incorporated MOF, $[Co_2(ndc)_2(bipyene)] \cdot C_6H_6 \cdot H_2O$, all the attempted syntheses using other guest molecules also failed to produce MOFs with entrapped guest molecules. Apparently, in addition to the hydrophobic interactions between the guest molecules and the frameworks, the inclusion of a guest molecule into the framework of a MOF requires additional conditions, such as the size and shape compatibility, to be satisfied. However, these compatibility conditions are hard to predict because the structures of MOFs are highly unpredictable unless specially designed ligands are used. At any rate, our results show that the idea of incorporating hydrophobic molecules into hydrothermal system is a possible means to create porous MOFs even

(20) (a) Liu, Y.-H.; Lin, C.-S.; Chen, S.-Y.; Tsai, H.-L.; Ueng, C.-H.; Lu, K.-L. *J. Solid State Chem.* **2001**, *157*, 166. (b) Livage, C.; Guillou, N.; Marrot, J.; Ferey, G. *Chem. Mater.* **2001**, *13*, 4387. (c) Livage, C.; Egger, C.; Ferey, G. *Chem. Mater.* **2001**, *13*, 410. (d) Noro, S.-I.; Kitaura, R.; Kondo, M.; Kitagawa, S.; Ishii, T.; Matsuzaka, H.; Yamashita, M. *J. Am. Chem. Soc.* **2002**, *124*, 2568. (e) Ayyappan, P.; Evans, O. R.; Lin, W. *Inorg. Chem.* **2002**, *41*, 3328. (f) Tong, M.-L.; Chen, H.-J.; Chen, X.-M. *Inorg. Chem.* **2000**, *39*, 2235. (g) Jiang, Y.-C.; Lai, Y.-C.; Wan, S.-L.; Lii, K.-H. *Inorg. Chem.* **2001**, *40*, 5320.

(21) (a) Papaefstathiou, G. S.; McGillivray, L. R. *Angew. Chem., Int. Ed.* **2002**, *41* (12), 2070. (b) Xu, X. L.; Nieuwenhuyzen, M.; James, S. L. *Angew. Chem., Int. Ed.* **2002**, *41* (5), 764. (c) Tao, J.; Yin, X.; Huang, R.; Zheng, L.; Ng, S. W. *Inorg. Chem. Commun.* **2002**, *5*, 975. (d) Sun, Z.-G.; Ren, Y.-P.; Long, L.-S.; Huang, R.-B.; Zheng, L.-S. *Inorg. Chem. Commun.* **2002**, *5*, 629.

(22) (a) Sun, W. Y.; Kusukawa, T.; Fujita, M. *J. Am. Chem. Soc.* **2002**, *124*, 11570. (b) Biradha, K.; Fujita, M. *Chem. Commun.* **2002**, 1866. (c) Kusukawa, T.; Fujita, M. *J. Am. Chem. Soc.* **2002**, *124*, 13576.

(23) *Treatability Manual, Vol. I, Treatability Data*; EPA-600/2-82-001a; Office of Research and Development, U.S. EPA: Washington, DC, 1983.

(24) (a) West, C. D.; Harwell, J. H. *Environ. Sci. Technol.* **1992**, *26*, 2324. (b) Park, J.-W.; Jaffe, P. R. In *Emerging Technologies for Hazardous Waste Management*: *1992 Book of Abstracts for the Special Symposium*; Tedder, D. W., Ed.; Industrial & Engineering Chemistry Division, American Chemical Society: Washington, DC, 1992; pp 620−623. (c) Kile, D. E.; Chiou, C. T. *Environ. Sci. Technol.* **1989**, *23*, 832.

under hydrothermal conditions. We believe that there will be many more examples to be found through exploratory syntheses employing various combinations of ligands and metal ions.

Conclusions

In this study, we have synthesized three different MOF compounds whose frameworks are composed of Ni(II), btc, and bpy ligands. While the reaction in pure water produces compound **2**, the addition of naphthalene in the reaction mixture gives rise to dramatic changes by forming MOFs with entrapped naphthalene (compounds **1** and **3**) or a different framework structure (compound **4**); that is, these MOFs have a different implication on the role of added naphthalene molecules. It is noteworthy that compound **2** is the only compound that forms regardless of the composition of the starting mixture when naphthalene is not added.

The successful syntheses of various crystal structures by adding naphthalene strongly suggest that even presently well-known MOF systems may have a new dimension of structural variability simply by modifying the solvent composition and the capacity of hydrothermal reactions can be extended in preparing novel organic−inorganic hybrid materials.

Acknowledgment. This work was financially supported by the Center for Nanotubes and Nanostructured Composites at SKKU.

Supporting Information Available: X-ray crystallographic files in CIF format for the structure determination of compounds **2**, **3**, and **4**. This material is available free of charge via the Internet at http://pubs.acs.org.

IC049030J